# Nanoscale

## Accepted Manuscript

This is an *Accepted Manuscript*, which has been through the RSC Publishing peer review process and has been accepted for publication.

*Accepted Manuscripts* are published online shortly after acceptance, which is prior to technical editing, formatting and proof reading. This free service from RSC Publishing allows authors to make their results available to the community, in citable form, before publication of the edited article. This *Accepted Manuscript* will be replaced by the edited and formatted *Advance Article* as soon as this is available.

To cite this manuscript please use its permanent Digital Object Identifier (DOI®), which is identical for all formats of publication.

More information about *Accepted Manuscripts* can be found in the **Information for Authors**.

Please note that technical editing may introduce minor changes to the text and/or graphics contained in the manuscript submitted by the author(s) which may alter content, and that the standard **Terms & Conditions** and the **ethical guidelines** that apply to the journal are still applicable. In no event shall the RSC be held responsible for any errors or omissions in these *Accepted Manuscript* manuscripts or any consequences arising from the use of any information contained in them.

## RSC Publishing

**www.rsc.org/nanoscale**
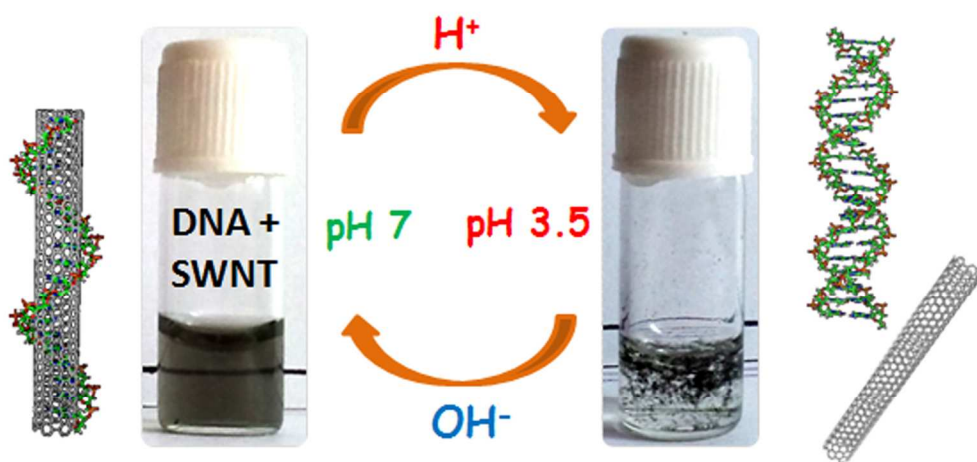
Role of DNA Secondary Structures in the Reversible Dispersion/Precipitation and Separation of Metallic and Semiconducting Single-walled Carbon Nanotubes
1047x531mm (72 x 72 DPI)

**ARTICLE TYPE**

# Role of pH Controlled DNA Secondary Structures in the Reversible Dispersion/Precipitation and Separation of Metallic and Semiconducting Single-walled Carbon Nanotubes

**Basudeb Maji,[a] Suman K. Samanta,[a,#] and Santanu Bhattacharya*[a,b,c]**

Single-stranded DNA (ss-DNA) oligomers ($dA_{20}$, $d[(C_3TA_2)_3C_3]$ or $dT_{20}$) are able to disperse single-walled carbon nanotubes (SWNTs) in water at pH 7 through non-covalent wrapping on the nanotube surface. At lower pH, an alteration of the DNA secondary structure leads to a precipitation of the SWNTs
10 from the dispersion. The structural change of $dA_{20}$ takes place from the single-stranded to the A-motif form at pH 3.5 while in case of $d[(C_3TA_2)_3C_3]$ the change occurs from the single-stranded to the i-motif form at pH 5. Due to this structural change, the DNA is no longer able to bind the nanotube and hence the SWNT precipitates from its well-dispersed state. However, this could be reversed on restoring the pH to 7, where the DNA again relaxes in the single-stranded form. In this way the dispersion and precipitation
15 process could be repeated over and over again. Variable temperature UV-Vis and CD spectroscopy studies showed that the DNA-SWNT complexes were thermally stable even at ~90 °C at pH 7. Broadband NIR laser (1064 nm) irradiation also demonstrated the stability of the DNA-SWNT complex against local heating introduced through excitation of the carbon nanotubes. Electrophoretic mobility shift assay confirmed the formation of stable DNA-SWNT complex at pH 7 and also the generation of DNA
20 secondary structures (A/i-motif) upon acidification. The interactions of ss-DNA with SWNTs cause debundling of the nanotubes from its assembly. Selective affinity of the semiconducting SWNTs towards DNA than the metallic ones enables separation of the two as evident from spectroscopic as well as electrical conductivity studies.

## Introduction

25 Hybrid materials developed from two or more components are particularly important because they often show combination of properties contributed by each one or sometimes even better performance.[1] Thus, when the individual component is a biopolymer such as single-stranded DNA or a nanomaterial such
30 as single-walled carbon nanotube (SWNT) respectively, the hybrid nano-bio-complexes often show superior biological as well as materials properties.[2] DNA has the ability to disperse SWNTs in water leading to the preparation of DNA-SWNT hybrid materials.[3] Indeed the DNA-SWNT hybrid materials have
35 been found to be useful for drug delivery,[4] biochemical sensing[5] and in the sorting of SWNTs.[6,7] Presence of DNA in the complex not only makes it bio-active but it also wraps the SWNT to make the resultant water-dispersible, primarily through stacking interactions of the DNA bases with the π-surface of the SWNTs.[8]
40 However, the secondary structures of DNA such as the single-stranded *vs.* the higher order organizations[9-11] are also crucial for their interaction with the SWNTs. Although duplex DNA,[9] triplex DNA[10] and i-motif[11] secondary structures are stabilized by SWNTs or its functionalized analogues due to specific
45 interactions, it can also cause precipitation of the SWNT from the dispersion due to aggregation. For instance, in case of covalently

attached DNA with SWNTs it is possible to induce aggregation of SWNTs through DNA mediated interactions.[12] Liu *et al.* and Kim *et al.* reported recently that covalently attached ss-DNA with
50 SWNT undergoes pH-induced reversible aggregation/dispersion in water by means of the formation of intermolecular i-motif structures by the C-rich ss-DNAs.[13] Lee *et al.* also reported covalent attachments of ss-DNA with functionalized MWNTs and their DNA-guided self-assembly process for carbon
55 nanotubes.[14] DNA oligonucleotides are also attached covalently on the patterned SWNT films to realize bio-sensing applications.[15]

Reversible non-covalent binding of DNA and SWNT and their decomplexation takes place through an interplay of electrostatic
60 and π-stacking interactions with the aid of externally added pyrene derivatives,[16] ethylenediamine[17] as well as $Ag^+$ and cysteine *etc.*[18] Recently Jung *et al.* has reported that addition of a complementary ss-DNA to the ss-DNA-SWNT hybrid induces a breakdown of the assembly leading to the precipitation of SWNT
65 through the formation of a double-stranded DNA.[19] Moreover, the process is irreversible, *i.e.,* the precipitated SWNT could not be dispersed again in the medium. The assembly of ss-DNA-SWNT through non-covalent means appeared as an effective platform for probing the biomolecular interactions.[20] However, it

is not known as to how the precipitated SWNT could be reverted back to the DNA-SWNT hybrid dispersion through non-covalent means. Such capability if accomplished could open up new opportunities for novel nano-bio-technological applications. Due to our interest, we investigated various types of nanomaterials.[21] Herein, we show the solubilization of SWNTs in water first by ss-DNA through non-covalent means and then a pH-induced reversible dispersion/precipitation of the SWNTs via crucial changes in the DNA secondary structure.

In the process it was also possible to separate the metallic and semiconducting SWNTs based on their selective affinity toward DNA. Although separation of metallic and semiconducting SWNTs were reported based on molecular charge transfer,[22] using scotch tape,[23] size-exclusion chromatography,[24] non-linear density-gradient ultracentrifugation,[25] gel chromatography[26] and via organic ligands through π-stacking interactions[27] *etc.,* the separation based on ss-DNA alone has not been achieved before. Therefore we report herein for the first time the pH-induced reversible dispersion/precipitation of SWNTs via alteration of secondary structure of DNA as well as the separation of metallic and semiconducting SWNTs. Although, the separation of metallic and semiconducting SWNTs have been achieved using anion exchange chromatography,[7] the process is considerably more cumbersome and expensive and the isolation of the individual components are difficult.[28] However, in the present approach, after the separation of metallic and semiconducting SWNTs, the individual components could be isolated conveniently just by changing the pH of the solution.

## Experimental Section

### A. Materials

All reagents were obtained from the best known commercial sources and were used as obtained. The oligonucleotides (HPLC grade) were purchased from Sigma. Their purity was confirmed using high resolution sequencing gel. The molar concentration of each ODN was determined from absorbance measurements at 260 nm based on their molar extinction coefficients ($\varepsilon_{260}$) 308000, 201000 and 148400 for $dA_{20}$, $d[(C_3TA_2)_3C_3]$ and $dT_{20}$ respectively. HiPco SWNT and deionized water were used in each experiment.

### B. Purification of HiPco SWNTs

The HiPco SWNT generally contains impurities like carbon-coated iron nanoparticles even upto ~30-35 wt%. The metal impurities have been removed by treatment with HCl-$H_2O_2$

following a reported procedure.[29] Briefly, a sample of HiPco SWNT was taken (20 mg) along with 20 mL of 1N hydrochloric acid solution and 20 mL of 30% $H_2O_2$ in a 250 mL round bottomed flask. The mixture was then heated at 65 °C with stirring for 4 h. After completion of every hour another batch of 20 mL of 1N hydrochloric acid and 20 mL of 30% $H_2O_2$ was added. This afforded a yellow colored solution with dark residue, which was stirred for another 1 h to decompose the remaining $H_2O_2$. Finally the SWNT was filtered out from this mixture and washed several times with deionized water and then air-dried to obtain 12 mg of SWNT. The purified SWNT was characterized with UV-Vis-NIR and Raman spectroscopy and transmission electron microscopy (TEM).

### C. Preparation of DNA-SWNT complexes

HiPco SWNT (0.1 mg) has been taken individually with 1 mL of 10 μM $dA_{20}$, $d[(C_3TA_2)_3C_3]$ (IM) or $dT_{20}$ DNA strand in water and heated at 95 °C for 5 min followed by snap chilling. Each mixture was then bath sonicated in an Elma Transsonic 460/H instrument at 35 W for 90 min under ice-cold condition. The partially dispersed SWNT mixture was then centrifuged at 13000 rpm for 60 min at 4 °C in a Hettich centrifugen mikro 22 R instrument. The clear, dark supernatant was carefully pipetted out as a black dispersion which remained stable for several months.

### D. Separation of DNA dispersible SWNTs from insoluble SWNTs

HiPco SWNT (0.3 mg) was dispersed in 3 mL of 10 μM DNA (either $dA_{20}$, IM or $dT_{20}$) in water in a micro-centrifuge tube which produced a black dispersion (referred as part A) and a black precipitate (part B) (Chart 1). The clear DNA-SWNT dispersion (part A) was acidified according to the DNA sequence used (*i.e.* pH 3.5 for $dA_{20}$, pH 5 for IM and pH 3 for $dT_{20}$). This led to the precipitation of the dispersed SWNT from each of the DNA-SWNT complex dispersions. The precipitated SWNT was then collected by centrifugation (13000 rpm, 5 min, 4 °C). The black precipitate was washed with deionized water and resuspended in 1 mL of 10 μM DNA and sonicated at 35 W for 30 min in ice-cold condition. The SWNT dispersion was then centrifuged at 13000 rpm for 30 min at 4 °C. This furnished a clear black dispersion leaving a very small insoluble part (15-20%) at the bottom. The transparent dispersion was pipetted out carefully and acidified followed by centrifugation to recover the dispersed SWNT. The black SWNT mass was then washed thoroughly with deionized water and air-dried. This was identified as DNA dispersible SWNT.
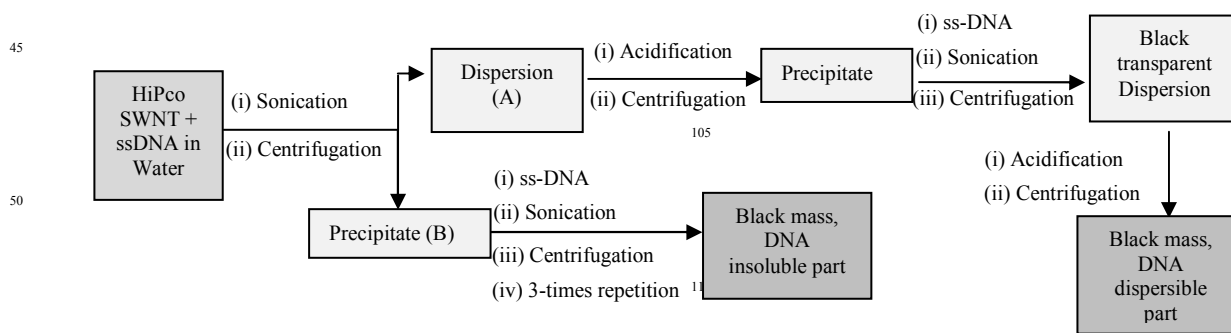


**Chart 1.** Flow chart depicting the process of separation of DNA dispersible SWNTs from insoluble SWNTs starting from as received HiPco SWNTs.

The insoluble part of SWNT (part B) obtained in the first step was treated with fresh 1 mL of DNA solution (10 μM strand concentration) to disperse the residual DNA dispersible SWNT. The process was repeated for 3 times to ensure the removal of any residual DNA dispersible SWNT. The residue that still remained insoluble was identified as the DNA insoluble SWNT.

### E. Raman Spectroscopy

Raman spectra of the SWNT samples were recorded with the help of a LabRAM HR high-resolution Jobin YvonHoriba HR 800 Raman spectrometer using a He–Ne laser ($\lambda_{ex}$ = 633 nm).

### F. UV-Vis-NIR and Circular Dichroism (CD) spectroscopy

UV-Vis-NIR absorption spectra of the dispersions were recorded on a Perkin-Elmer Lambda 35 UV-Vis spectrometer. CD spectra were recorded on a Jasco J-810 CD spectropolarimeter with a 10 mm path length. Contribution of the linear dichroism (LD) was excluded by recording the spectra with both sides of the quartz cell which showed no significant changes. All the spectra were recorded in 10 mM sodium cacodylate buffer medium. For variable temperature studies, UV-Vis and CD instruments were connected with peltier temperature controller system and each spectrum was recorded before equilibrating the system for 2-3 minutes.

### G. Transmission Electron Microscopy

Diluted dispersion of each sample was drop-cast onto a carbon-coated copper grid (200 mesh size) and the TEM images were taken at an accelerating voltage of 200 kV using TECNAI T20 instrument.

### H. Atomic Force Microscopy

A diluted dispersion of the samples was drop-cast on freshly cleaved mica substrates and it was air-dried. Images were recorded using a JPK Instrument NanoWizard JPK 00901 AFM instrument. Non-contact mode imaging was undertaken in air using silicon cantilevers of resonance frequencies of 260 kHz and a nominal tip radius of curvature of 10-15 nm.

### I. Zeta-potential Studies

Zeta-potential was measured with the deionized water samples in a ZetaPALS (Zeta potential analyzer) instrument from Brookhaven Instruments Corporation.

### J. Electrophoretic Mobility Shift Assay (EMSA)

The 21-mer ss-DNA sequences (IM), $dA_{20}$ and $dT_{20}$ were labeled with [γ-$^{32}$P]ATP (Amersham) at the 5'-end and purified by chromatography on Sephadex G-50 followed by 15% PAGE with 0.5X TBE running buffer at 120 V for 8 h. The required band was transferred to a centrifuged tube and eluted in TE buffer at pH 7.4 to get the labeled oligomer which was then mixed with unlabeled oligomer for further experiments. Both the DNA solutions containing respective labeled DNA were used to prepare the $dA_{20}$-SWNT and IM-SWNT complexes following the protocol discussed above under 'Preparation of DNA-SWNT complexes' section. The labeled DNA (20 μL) and the DNA-SWNT complex solutions were mixed with 5 μL of 10X agarose dye and electrophoresed against 80 V for 8 h on 15% polyacrylamide gel. On the other hand the $dA_{20}$-SWNT and IM-SWNT complex

solutions were acidified to pH 3.5 and pH 5 respectively and centrifuged to get the supernatant. The supernatant was mixed with 10X agarose dye and electrophoresed keeping the $dT_{20}$ as reference on 15% polyacrylamide gel with 20 mM sodium cacodylate running buffer of either pH 3.5 or pH 5.0 at 80 V for 8 h. The gels were then dried and visualized using Fuji-5000 phosphorimager.

### K. Current (*I*)-Voltage (*V*) Measurements

The SWNT containing samples were drop-cast on separate gold sputtered glass plates having an electrode gap of 30 μm, and allowed to air-dry in a dust free environment. The *I-V* characteristics of each sample were measured in a two-probe electrode using a PM5 Probe station, Agilent Device Analyzer B1500A instrument.

## Results and discussion

### A. Purification of SWNTs

Commercially available HiPco SWNT which generally contains metallic impurities like carbon-coated iron nanoparticles *etc.* were first purified using HCl-$H_2O_2$ treatment (*c.f.* Experimental Section).[29] The integrity of the nanotubes remains intact during the purification process as evident from transmission electron microscopy (TEM) and Raman spectra. The nanoparticle impurities present with the SWNTs were removed in the purification process as clearly visible under the TEM images (Fig. 1a,b). However, the tubes still remained in an aggregated state. Raman shift of the RBM band (radial breathing mode) between 150-300 cm$^{-1}$, G-band (~1590 cm$^{-1}$), D-band (~1335 cm$^{-1}$) and 2D-band (~2670 cm$^{-1}$) remained almost unaltered before and after the purification process (Fig. S1†).
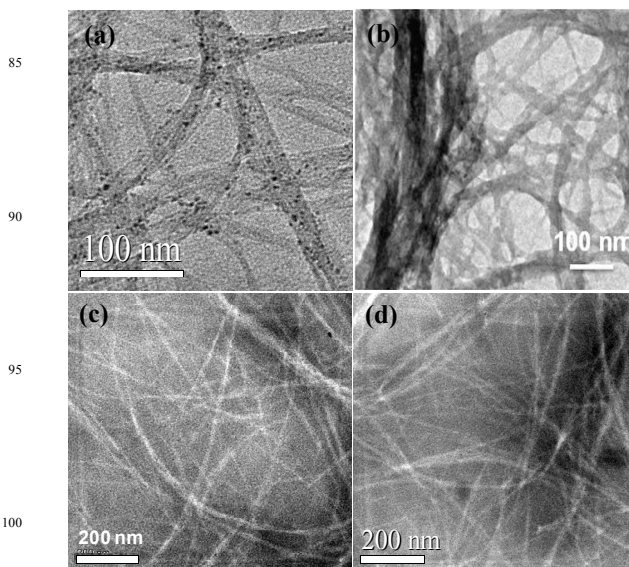


**Fig. 1.** TEM images showing bundles of SWNT (a) before purification, (b) after purification and dispersed SWNT with oligonucleotides (c) $dA_{20}$ and (d) IM.

### B. DNA induced Solubilization of SWNTs

Purified SWNT was dispersed in deionized water with the aid of three different oligo-deoxynucleotides (ODNs), $dA_{20,}$

d[(C$_3$TA$_2$)$_3$C$_3$] (abbreviated as IM) or dT$_{20}$. An inhomogeneous mixture of DNA and SWNT in water was rapidly transformed into a transparent dispersion upon brief sonication (Fig. 2b,c). The resulting dispersion did not precipitate on aging for more than six months. UV-Vis-NIR studies of the DNA-SWNT complexes with either dA$_{20}$ or IM show an absorption maximum ($\lambda_{max}$) at ~260 nm (Fig. 2a and Fig. S2†) which is similar to the $\lambda_{max}$ of the individual DNA (10 μM in each case). Presence of the semiconducting band (S$_{22}$) at 700-1000 nm and the metallic band (M$_{11}$) at 500-700 nm confirmed the dispersion of SWNTs in the DNA solution.[30] Stability of the resulting DNA-SWNT hybrid was measured with the help of zeta potential, the value of which appeared within -30 to -40 V (Fig. S3†). This indicated a reasonably good stability of the hybrid system.[31]
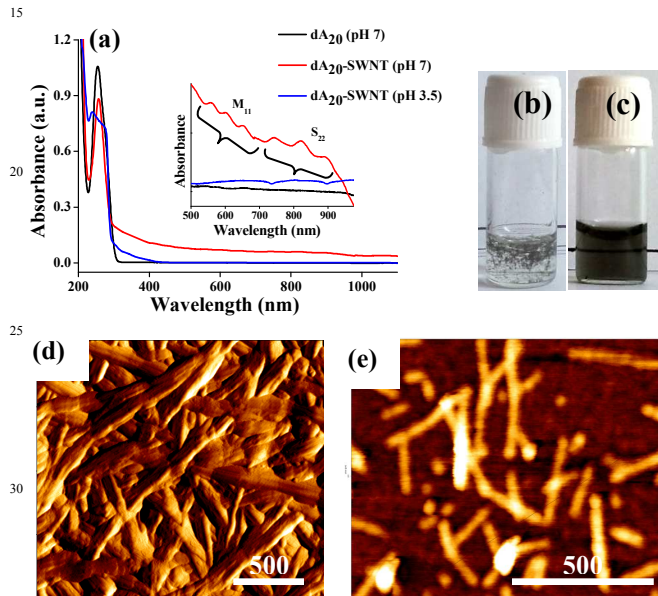


**Fig. 2.** (a) Absorption spectra of dA$_{20}$ alone and SWNT complex at pH 7 and 3.5, inset showing magnified spectra from 500-1000 nm. The images show addition of SWNTs (0.1 mg) into the solution of dA$_{20}$ (10 μM) in water (b) before and (c) after sonication, AFM images of (d) purified SWNT alone and (e) dA$_{20}$-SWNT complex.

Atomic force microscopy (AFM) images showed the presence of high-aspect ratio nanotubes present in bundles in the purified SWNT samples (Fig. 2d,e and Fig. S4†). However, in the DNA-SWNT hybrid, the nanotubes were found to be well separated in suspension. In both the DNA-SWNT hybrids (of either dA$_{20}$ or IM), the individual nanotubes were clearly visible with an average length of ~400-500 nm and ~40-60 nm in diameter. The height image along the surface of the nanotube was found to be considerably uneven probably due to the wrapping with the DNA (Fig. S5b,c†). Transmission electron microscopy (TEM) images were also recorded for the DNA treated SWNTs and were compared to that with purified SWNTs. TEM images clearly showed efficient debundling of the individual SWNTs distributed throughout the sample (Fig. 1c,d).

**C. Effect of pH**

We investigated the effect of pH on the structural alteration of DNA and the stability of DNA-SWNT hybrids using circular dichroism (CD) spectroscopy. A-rich ODNs (dA$_n$) which remain as single-stranded at neutral pH could potentially associate via AH$^+$-H$^+$A base pairing to form A-motif DNA at acidic pH (<4.5) (Fig. S6a†).[32,33] Thus, at pH 7, the CD spectrum of dA$_{20}$ showed a weak positive band at 275 nm, a negative band at 250 nm and a strong positive band at 217 nm with a shoulder at 232 nm which is a characteristic of the CD signature of ss-dA$_{20}$ (Fig. 3a).[32,33] Upon acidification of the medium, the intensity of the 275 nm band increased and that of the 217 nm band decreased while the 250 nm band showed a hypochromic blue-shift to 242 nm. These spectral changes indicate a structural alteration of dA$_{20}$ from the single-stranded to the A-motif form (Fig. 3a).

CD spectra of the DNA-SWNT hybrids were recorded to investigate the influence of SWNTs on the structural alterations of DNA at different pH of the media. The dA$_{20}$-SWNT hybrid showed CD signature similar to that of ss-dA$_{20}$ at pH 7 where the complex remained dispersed in water indicating that the interaction of SWNTs with DNA did not lead to any structural changes at this pH (Fig. 3b). However, an interesting phenomenon occurred when the pH of the medium was decreased. At a lower pH (3.5), SWNTs precipitated from the DNA-SWNT dispersion (Fig. 3c). This indicates that at pH 3.5, a structural alteration of dA$_{20}$ takes place from the single-stranded to the A-motif form even when the DNA is wrapped around SWNTs. Thus, the A-motif form is unable to bind SWNTs and therefore it got precipitated at pH 3.5 while the single-stranded form could bind and disperse SWNTs at pH 7. The absorption spectral bands due to M$_{11}$ and S$_{22}$ of SWNTs also disappeared indicating that the nanotubes were not present in the dispersed state in the acidified solution (Fig. 2a). The CD spectrum at pH 3.5 resembled the one recorded for dA$_{20}$ alone at the same pH. The intensity of the strong positive band at 217 nm diminished along with an increase in the intensity of the 275 nm band (Fig. 3d). Also, the negative band at 250 nm shifted to 242 nm which resembled the CD signature of the A-motif DNA.[34] These phenomena indicate that the structural integrity of DNA was not destroyed throughout the SWNT dispersion and the acidification process.

When we restored the pH back to 7, the precipitated SWNTs could be readily dispersed merely by gentle shaking the vial which reproduced the initial transparent dispersion. Moreover, the CD signature matched again with that of the dA$_{20}$-SWNT complex recorded at pH 7. This phenomenon was found to be fully reversible for a number of cycles with respect to the changes in pH (Fig. 3d). This indicates a reversible nature of association and dissociation of the SWNTs with dA$_{20}$ depending on the pH induced changes in the structure of DNA. The above phenomenon is depicted graphically in Fig. 4. At pH >4.5 each of the bases of dA$_{20}$ are likely to stay in the non-protonated state and thus DNA exists as a single-stranded form. Therefore, sonication of the mixture leads to the solubilization of SWNTs by the wrapping of dA$_{20}$ on the SWNT surface. However, on acidification (pH ≤4.5) the DNA bases are protonated and two individual dA$_{20}$ strands form a duplex A-motif structure through the H-bonding between the self-complementary base-pairs.[32,33] Therefore, the dominating H-bonding interactions between the individual DNA strands lead to the decomplexation of the DNA-SWNT complex which is assembled via the weaker π-stacking interactions.
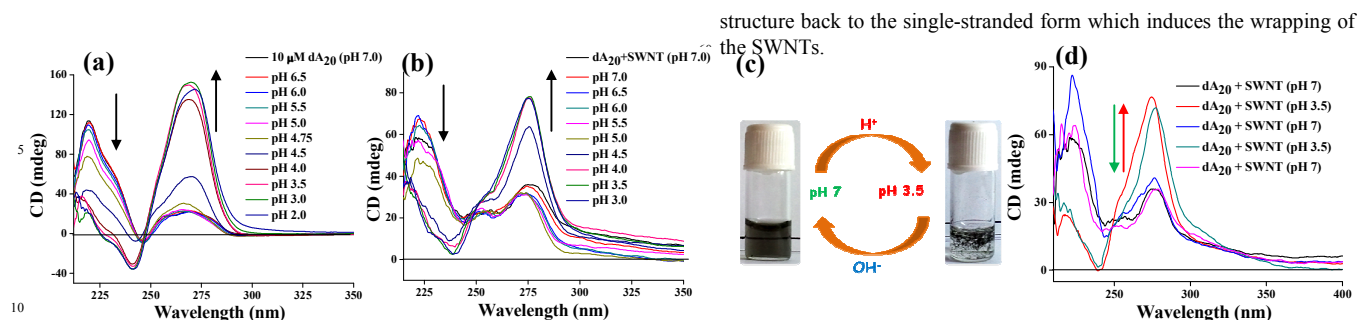
**Fig. 3.** CD spectra of dispersion of (a) dA$_{20}$ and (b) dA$_{20}$-SWNT hybrid at different pH in water. Reversible responses of the pH variation on the DNA-SWNT hybrids as shown using (c) Photographic images and (d) CD studies.

The pH dependent quadruplex DNA structure formation from the C-rich ODNs like human telomeric sequence d[(C$_3$TA$_2$)$_3$C$_3$] (IM) has been also reported due to the formation of i-motif.[35] The partial protonation of the cytosine bases leads to the intercalation of the C-C$^+$ pairs of two parallel-stranded duplex and thus generates an intramolecular i-motif structure at slightly acidic pH (<6.5) (Fig. S6b†). Like dA$_{20}$, IM is also efficiently dispersed SWNT in water at pH 7 and the dispersed SWNT precipitated at lower pH (≤5). Moreover, this phenomenon was reversible upon changes in pH. The CD spectra of IM and IM-SWNT hybrid showed quite similar signatures indicating that the random single-stranded structures of IM remained intact in the hybrid (Fig. 5). Upon acidification (pH 5), the DNA could no longer hold the SWNT in dispersion. A positive band at 276 nm intensified with 10 nm red-shift along with the appearance of a negative band at 250 nm which is consistent with the characteristics of i-motif structure formation.[36] Restoration of the pH back to 7 led to the dispersion of the precipitated SWNTs along with the transformation of the CD spectrum from the i-motif to that of a single-stranded structure (Fig. 4). Thus, CD spectroscopy has been used to correlate the pH-induced visual changes in the DNA-SWNT suspension with the morphological changes in the DNA structure. These studies provide unambiguous evidence to claim that SWNT precipitation and formation of DNA secondary structures (A/i-motif) occur simultaneously.
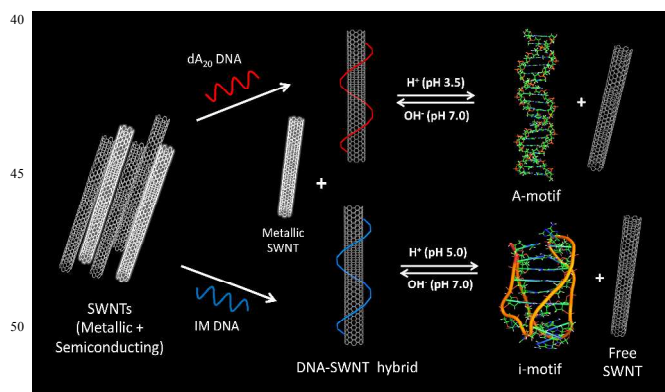


**Fig. 4.** Schematic representation (not to scale) showing reversible DNA induced dispersion and precipitation of SWNTs based on pH-mediated single-stranded *vs.* A-motif or i-motif structure formation. Sonication induces DNA wrapping on the SWNT surface which on acidification leads to the disassembly and an A-motif structure is formed from dA$_{20}$ while IM forms the i-motif. Increasing the pH again alters the DNA

structure back to the single-stranded form which induces the wrapping of the SWNTs.
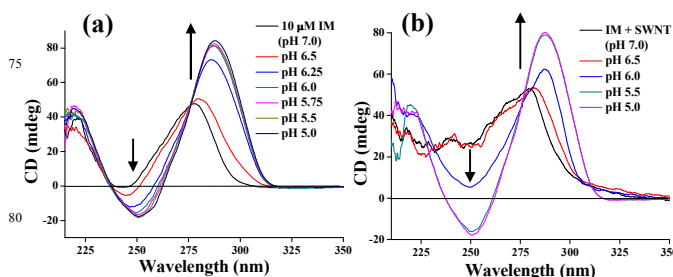


**Fig. 5.** CD spectra of the dispersion of (a) IM and (b) IM-SWNT hybrid at different pH in water.

The role of ss-dT$_{20}$ DNA sequence in SWNT dispersion was also investigated at various pH values in aqueous media. The dT$_{20}$-SWNT complex was found to be stable as dispersion in water over a wide range of pH from 10.0 to ~5.0. However, further decrease in pH rendered the complex unstable and at ~pH of 3.0, precipitation started to occur (Fig. S7b†). Upon decreasing the pH below 9.9, the deprotonated form of the thymine nucleobases in dT$_{20}$ started getting protonated.[37a] Further acidification probably promotes the formation of the O4-H enol form as shown (Fig. S8a†). This leads to the development of partial positive charge at N1, C6, C5 and C4 of the thymine bases.[37b] Due to the absence of any other protonation sites in thymine, formation of cationic nucleobases in dT$_{20}$ is however, not feasible. Apart from the nucleobases, other protonation sites exist with the anionic phosphate backbone. The phosphodiester moiety has p$K$a in the range of ~1-3,[37c,d] depending upon various parameters like temperature, electrolyte, ionic strength and dielectric constant of the medium *etc.*[37e] Thus, at a very low pH, the ionization equilibrium of phosphodiester backbone may get altered. This change in the ionic state may affect the SWNT dispersion ability of dT$_{20}$ DNA which may be responsible for the breakdown of dT$_{20}$-SWNT complex at a low pH (pH 3.0 or below). It may be noted that the protonation of the phosphate backbone should not play any role in the case of dA$_{20}$-SWNT and IM-SWNT complexes as they precipitate out already at higher pH (pH 4 and 5.5 respectively) whereas dT$_{20}$-SWNT remained as stable dispersion under such conditions.

In summary, DNA sequence capable of forming secondary structures via protonation of nucleobases (Fig. S8b,c†) resulted in the precipitation of SWNTs at or around their p$K$a. Whereas the

DNA sequence which could not form any DNA secondary structure carrying negatively charged nucleobases ($dT_{20}$ at pH 10.0) was still able to disperse SWNTs in aqueous media unless the ionic state of the anionic phosphate backbone is disturbed (at pH 3.0). This observation clearly suggests that only ionization of nucleobases may not be enough to disintegrate the DNA-SWNTs complex. Thus, these control experiments further confirm that DNA secondary structures (A-motif and i-motif) have significant role in the dispersion and precipitation of SWNTs in the aqueous medium.

Interestingly, the restoration of pH back to 7 (from pH 3) did not result in complete dispersion of the precipitated SWNTs (Fig. S7c†) as most of the precipitate had settled down. This result again indicates that $dT_{20}$-SWNT complex formation is not so facile as compared to $dA_{20}$-SWNT and IM-SWNT. However, a brief sonication of the pH restored mixture of $dT_{20}$-SWNT and buffer resulted in the formation of a stable dispersed state in the aqueous medium (Fig. S7d†). The stability of the $dT_{20}$-SWNT complex at different pH has also been probed using UV-Vis-NIR spectroscopy (Fig. S9a†) which explains the observed changes.

To further verify the role of pH we have also determined the p$K$a of the adenine bases in $dA_{20}$ before and after complexation with SWNT using CD titration data.[32,33] A first-order derivative of CD intensity *vs.* pH plot revealed the p$K$a of $dA_{20}$ alone and the hybrid at ~4.5 and ~4.0 respectively (Fig. S10†). Similarly, the p$K$a of IM and IM-SWNT appeared at ~6.5 and ~6.0 respectively. The p$K$a values determined for the DNA alone are in good agreement with the literature reports.[23,36] These results clearly indicate that the formation of the A/i-motif from the DNA-SWNT hybrid is less favorable than the free ODNs which are compensated by more number of $H^+$ ions in the solution.

### D.  Electrophoretic Mobility Shift Assay (EMSA)

The preparation of DNA-SWNT complex and the formation of DNA secondary structure from the complex has been investigated with the help of electrophoretic mobility shift assay (*c.f.* Experimental Section). The electrophoresis demonstrated that IM (21-mer) at pH 7 has almost similar mobility with that of $dT_{20}$ (20-mer) indicating the single-stranded nature of IM (Fig. 6, lane III). Slightly higher mobility of the 21-mer IM may be possibly due to the intra-strand interaction which gives to some extent higher compactness than that of $dT_{20}$. The IM-SWNT complex under electrophoretic condition could not penetrate the polyacrylamide gel and thus remained confined in the well whereas the DNA alone could move easily under similar conditions (Fig. 6, lane IV, V). Importantly, the band of higher mobility corresponding to the ss-DNA was almost absent in case of IM-SWNT indicating efficient wrapping of DNA on SWNT and absence of free DNA in the solution (Fig. 6, lane V). Furthermore, the electrophoretic assay of IM-SWNT complex at pH 5 showed a single band of even higher mobility than the $dT_{20}$ marker indicating formation of a highly compact, intramolecular tetraplex DNA structure which matches with the preformed i-motif DNA mobility (Fig. 6, lane VII, VIII).[11]

On the other hand, the $dA_{20}$ sequence which showed almost similar mobility with $dT_{20}$ at pH 7 (Fig. 6, lane II), generated a band of significantly lower mobility upon acidification of $dA_{20}$-SWNT complex. The band of lower mobility resembles the formation of a higher molecular weight intermolecular duplex

DNA structure known as A-motif (Fig. 6, lane X). The electrophoretic mobility shift assay thus gave a strong evidence towards the single-strand DNA mediated complex formation and the generation of secondary DNA structure upon acidification which is becomes inefficient to disperse SWNTs in the solution.
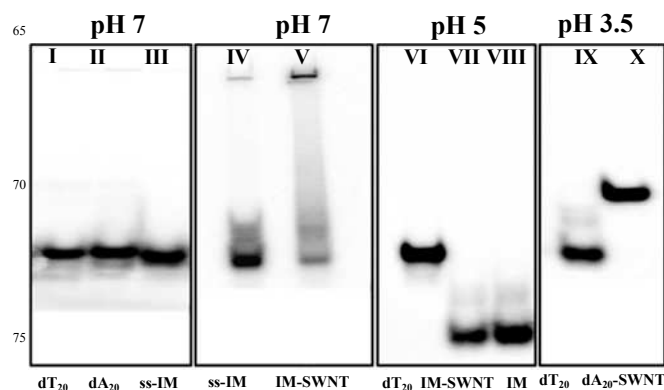


**Fig. 6.** Electrophoretic mobility shift assay of DNA and DNA-SWNT complexes. EMSA. lane (I): $dT_{20}$ marker; lane (II): $dA_{20}$ at pH 7; lane (III): IM at pH 7; (IV) IM at pH 7; lane (V): IM-SWNT at pH 7; lane (VI): $dT_{20}$ marker; lane (VII): IM-SWNT at pH 5; lane (VIII): IM at pH 5; lane (IX): $dT_{20}$ marker and lane (X): $dA_{20}$-SWNT at pH 3.5.

### E.  Thermal stability of the DNA-SWNT complexes

Though both the DNA sequences were shown to have efficient SWNT dispersion capability, it was important to investigate the stability of the DNA-SWNT complexes. Variable temperature UV-Vis and CD spectroscopic studies were undertaken to elucidate their thermal properties (Fig. 7 and Fig. S11†). Variable temperature UV-Vis spectroscopy of DNA-SWNT dispersion at pH 7 showed the presence of characteristic van Hove singularities even at high temperature (~90 °C) (Fig. 11a). As DNA is most likely to be present in a single-stranded random fashion at this pH, no structural transition was expected with the rise in temperature except the decomplexation of the DNA-SWNT complexes. However, precipitation of the dispersed SWNTs was not observed at this temperature and the absorption spectra showed a signature resembling DNA-SWNT hybrid. This indicates strong association and thermal stability of the DNA-SWNT complexes.

To further investigate, we also performed an NIR broadband laser (1064 nm, 3 W, LSR 1064H-3W, Laserver) induced irradiation of the DNA-SWNT complex dispersion. Because of the presence of the SWNT in such complexes, the dispersion gets heated up as was reported earlier (Fig. S12, S13†).[2f] Interestingly, even after 30 min of NIR irradiation, it did not result in any precipitation of the SWNT from the DNA ($dA_{20}$, IM or $dT_{20}$) bound dispersion in water. The total absorption of the laser beam by the DNA-SWNT dispersion indicates the presence of significant amount of SWNTs in the medium (Fig. S12, bottom†). The high intensity irradiation also resulted in considerable elevation of the temperature (~75 °C) (Fig. S13†). This observation further confirms the thermal stability of the DNA-SWNT complexes.

Acidification of the DNA-SWNT complex dispersions to pH near the respective protonation p$K$a of DNA showed immediate

precipitation of the dispersed SWNTs with a sharp change in their CD signature (Fig. 3 and Fig. 5). Variable temperature UV-Vis
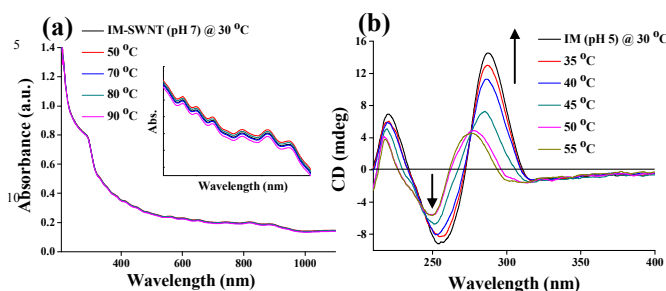
**Fig. 7**. Variable temperature (a) UV-Vis spectroscopy of IM-SWNT complex at pH 7 and (b) CD spectroscopy of IM alone at pH 5.0 (i-motif).

and CD spectroscopy enabled us to determine the denaturing temperature of the secondary DNA structures formed upon acidification. This also addresses the driving force for the DNA-SWNT complex formation as well as the formation of the DNA secondary structure upon acidification. Under CD spectroscopy, the A-motif DNA was shown to have very high melting temperature of ~85 °C whereas the i-motif structure showed a considerably lower melting temperature (~42 °C) (Fig. S11b,c and S11f†) which was consistent with the thermal denaturation temperature determined from UV-Vis spectroscopy (Fig. S11d,e†).[35] Therefore, the thermal stability of the DNA-SWNT complexes (at pH 7) is higher than that of the free DNA secondary structures under acidic conditions. Surprisingly, the IM-SWNT complex which showed high thermal stability even at 90 °C (at pH 7) generates a secondary structure (i-motif) having notably lower thermal stability (~42 °C) upon acidification (at pH 5). Therefore, generation of a less stable structure from a more stable one could be explained considering the fact that the DNA oligomer has an anionic phosphate-sugar chain along with hydrophobic nucleo-bases which show amphiphilic property. The hydrophobic nitrogen bases are stacked onto the nanotube aromatic backbone via $\pi$-$\pi$ interaction and the hydrophilic phosphate-sugar backbone are exposed to water. Thus a hydrophobic material (*e.g.* SWNT) can be appropriately wrapped by DNA to hide the same from the aqueous media to form a stable dispersion.

However, the protonation of the hydrophobic nitrogenous-bases at lower pH makes a significant change in the ionization and nature of the DNA. Most likely the protonated nitrogenous-bases become considerably inefficient towards the interaction with the hydrophobic carbon nanotubes. The strong association of the DNA-SWNT complex thus brakes down to a significant extent. Moreover, the formation of the secondary structure at lower pH facilitates the dissociation. Thus, not the formation of DNA secondary structure alone but a loss in efficient SWNT interaction with protonated forms of DNA also leads to the decomplexation of the DNA-SWNT complex in an acidic medium (Fig. S14†).

## F. Separation of Semiconducting and Metallic SWNTs

For the solubilization of SWNT with ss-DNA, 0.3 mg of purified HiPco SWNT was mixed with 3 mL of 10 µM ss-DNA ($dA_{20}$, IM or $dT_{20}$) and the mixture was sonicated followed by centrifugation. After a careful separation process (*c.f.* Experimental Section), the SWNT obtained from the DNA dispersion and the insoluble parts were collected separately and characterized using UV-Vis-NIR absorption and Raman spectroscopy. Raman spectrum of the purified HiPco SWNT showed the characteristic RBM bands at ~190 and 210 cm$^{-1}$ due to the presence of semiconducting and metallic SWNTs respectively[38] where the intensities of both the bands appeared to be almost equal to each other (Fig. 8a). However, the DNA dispersed SWNTs showed a greater intensity of the 190 cm$^{-1}$ band. In contrast, the DNA insoluble SWNTs showed that the intensities of the 210 and 253 cm$^{-1}$ bands were greater compared to the 190 cm$^{-1}$ band. The other two characteristic Raman band appears at 1500-1600 cm$^{-1}$ (G$^+$-band and G$^-$-band). The DNA dispersible SWNTs exhibits two bands at 1589 and 1557 cm$^{-1}$ which are quite characteristic of the semiconducting SWNT. On the other hand, the DNA insoluble SWNTs shows bands at 1584 and 1546 cm$^{-1}$ which are consistent with the signature of the metallic SWNTs.[22] This indicates that there is an enrichment of the semiconducting nanotubes in the DNA dispersed part while the DNA insoluble part contains mostly metallic SWNTs.[22,28]

UV-Vis-NIR absorption spectra revealed that the intensity of $M_{11}$ band at 500-700 nm and $S_{22}$ band at 700-1000 nm increased in the DNA insoluble and dispersible SWNTs respectively (Fig. 8b). The characteristic van Hove singularities corresponding to the nanotubes of different chirality (m,n) indicate the presence of both metallic and semiconducting tubes in the purified HiPco SWNTs. The DNA dispersible part showed enhancement in the semiconducting band intensity corresponding to the chirality of
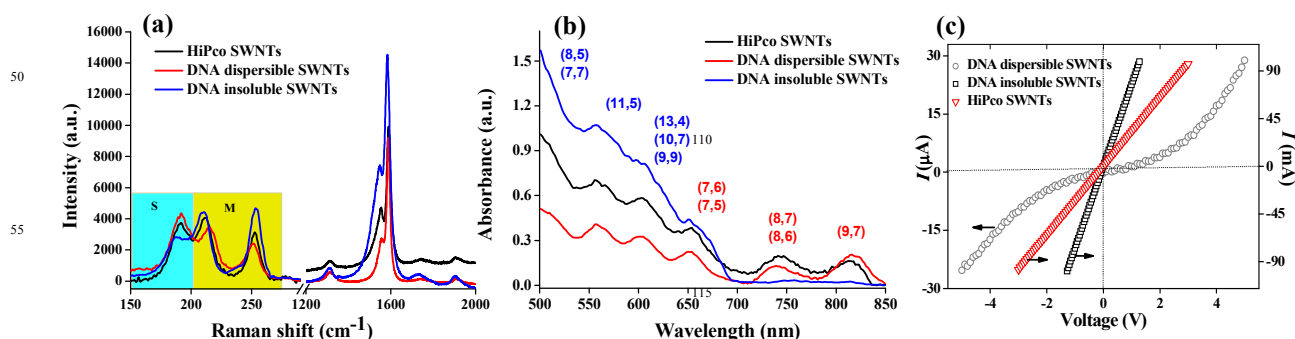


**Fig. 8.** (a) Raman spectra and (b) Absorption spectra of HiPco SWNT, $dA_{20}$-solubilized SWNT and $dA_{20}$-insoluble SWNT (solubilized with 1% SDS). ⊺[DNA] = 10 µM. (c) Electrical conductivity studies (*I-V* measurements) of HiPco SWNT, DNA dispersed SWNT and the precipitated SWNT from DNA solution. The notations, 'S' and 'M' in Fig. 8 (a) denote characteristic Raman spectral signatures due to semi-conducting and metallic forms of SWNT.

(8,7), (8,6) and (9,7) nanotubes whereas the DNA insoluble part showed enhancement in the metallic band intensity corresponding to the chirality of (8,5), (7,7), (11,5), (13,4), (10,7) and (9,9) nanotubes.[39]

Electrical conductivity (current-voltage) measurements confirmed the semiconducting behavior (non-linear *I-V* curve) of the DNA dispersible SWNTs while a metallic behavior (linear *I-V* curve) was evident from the insoluble part (Fig. 8c and Fig. S15†).[22] The purified HiPco SWNT also showed significant metallic behavior which could be due to the presence of highly conducting metallic tubes along with the semiconducting ones. However, the DNA insoluble SWNT showed even higher conductivity than the purified HiPco SWNTs.

Therefore, these results suggest that the DNA has a preferential affinity towards semiconducting SWNTs over metallic ones. It is reported that a DNA-SWNT complex which results in higher HOMO-LUMO energy gap leads to a chemically more stable complexation.[40] Therefore, a complex of DNA and semiconducting SWNTs having higher HOMO-LUMO energy gap may be responsible for the preference over the metallic SWNTs in terms of complexation. Few organic ligands with large π-aromatic surface were also known to bind selectively with the semiconducting SWNTs and thus result in a separation from the metallic ones.[22,27] The molecular charge-transfer between SWNTs and π-system of the organic ligands exhibit selectivity in the interaction of electron-donor and acceptor aromatic surface with SWNTs. The nucleobases present in DNA also offer π-aromatic surface attached to the anionic phosphate backbone which might induce selective charge-transfer interaction and preference towards the semiconducting SWNTs. Although, the separation of semiconducting and metallic SWNTs from a mixture was achieved through various means,[28,41] it was never demonstrated earlier through a preferential interaction of SWNTs with the ss-DNA.

## Conclusions

In summary, a facile dispersion of SWNTs was achieved in water through the interaction of single-stranded DNA ($dA_{20}$ or IM) at pH 7 via the wrapping of ss-DNA on the SWNT surface. Upon lowering the pH to ≤4 or ≤5.5 a structural alteration of the DNA (from ss- to A/i-motif) led to the precipitation of the SWNTs. However, raising the pH to 7 reverted the precipitated SWNTs back into DNA dispersion in both the cases. The process can be repeated several times and is thus fully reversible in nature. The advantage of such nucleic acid mediated reversible solubilization of SWNTs as a function of pH is obvious as the pH changes bring about specific secondary structural motifs depending on their base pairing propensity.

Preferential interaction of DNA with the semiconducting SWNTs than the metallic ones led to a separation of the two from a mixture. DNA mediated separation of SWNT components aided by pH induced changes in DNA secondary structures may be a useful technique because it is simple, reproducible and short. Such pH induced dispersion and precipitation of SWNT from its complexes mediated by synthetic ligands has so far not been reported. Moreover, while synthetic aromatic ligand based separation of SWNT components needs ligand concentration in the millimolar range, the DNA based separation procedure as described here needs only DNA in the micromolar concentration.

The possibility of designing appropriate DNA sequences generating different DNA topological structures promoted by various experimental stimuli (pH, ions, temperature *etc.*) may further extend the scope and thus open up another dimension. The methodology in which pH induced peeling off DNA from the SWNT surface using simple acid therefore enables one in isolating metallic form of SWNTs from the semiconducting SWNTs from their mixtures in the most convenient way.

## Notes and references

*aDepartment of Organic Chemistry, Indian Institute of Science, Bangalore 560012, India. Fax: +91-80-23600529; Tel: +91-80-22932664; E-mail: sb@orgchem.iisc.ernet.in*
*bJawaharlal Nehru Centre for Advanced Scientific Research Bangalore 560064, India.*
*cJ. C. Bose Fellow, Department of Science and Technology, New Delhi, India.*
*#Present address: Makromolekulare Chemie, Bergische Universitat Wuppertal, Gaussstrasse 20, 42119 Wuppertal, Germany.*

† Electronic Supplementary Information (ESI) available: Additional UV-Vis-NIR absorption, CD and Raman spectra, Zeta potential, AFM, laser irradiation and electrical conductivity data (S1-S15). See DOI: 10.1039/b000000x/

1    (a) S. R. Shin, C. K. Lee, S. H. Lee, S. I. Kim, G. M. Spinks, G. G. Wallace, I. So, J.-H. Jeong, T. M. Kang and S. Kim, *Chem. Commun.,* 2009, 1240-1242; (b) X. Li, Y. Peng, J. Ren and X. Qu, *Proc. Natl. Acad. Sci. USA,* 2006, **103**, 19658-19663; (c) S. K. Samanta, K. S. Subrahmanyam, S. Bhattacharya and C. N. R. Rao, *Chem. Eur. J.,* 2012, **18**, 2890-28901; (d) S. K. Samanta, A. Gomathi, S. Bhattacharya and C. N. R. Rao, *Langmuir,* 2010, **26**, 12230–12236; (e) N. Songmee, P. Singjai and M. in het Panhuis, *Nanoscale,* 2010, **2**, 1740–1745; (f) H. Ali-Boucetta, K. T. Al-Jamal, D. McCarthy, M. Prato, A. Bianco and K. Kostarelos, *Chem. Commun.*, 2008, **4**, 459-461; (g) L. Lara, S.Raffab, M. Pratoc, A. Biancod and K. Kostarelos, *Nanotoday,* 2007, **2**, 38-43.
2    (a) S. K. Misra, P. Moitra, B. S. Chhikara, P. Kondaiah and S. Bhattacharya, *J. Mater. Chem.,* 2012, **22**, 7985-7998; (b) R. Yang, X. Yang, Z. Zhang, Y. Zhang, S. Wang, Z. Cai, Y. Jia, Y. Ma, C. Zheng, Y. Lu, R. Roden and Y. Chen, *Gene Ther.,* 2006, **13**, 1714-1723; (c) S. Bhattacharya, D. Roxbury, X. Gong, D. Mukhopadhyay and A. Jagota, *Nano Lett.* 2012, **12**, 1826-1830; (d) B. S. Chhikara, S. K. Misra, S. Bhattacharya and *Nanotechnology* 2012, **23**, 065101; (e) Y. Li, X. Han and Z. Deng, *Angew. Chem. Int. Ed.*, 2007, **46**, 7481–7484; (f) S. K. Samanta, A. Pal, S. Bhattacharya and C. N. R. Rao, *J. Mater. Chem.,* 2010, **20**, 6881-6890; (g) A. Pal, B. S. Chhikara, A. Govindaraj, S. Bhattacharya and C. N. R. Rao, *J. Mater. Chem.,* 2008, **18**, 2593-2600; (h) R. Kumar, E. Gravel, A. Hagège, H. Li, D. V. Jawale, D. Verma, I. N. N. Namboothiri and E. Doris, *Nanoscale*, 2013, **5**, 6491-6497; (i) A. Kaniyoor, R. I. Jafri, T. Arockiadossa and S. Ramaprabhu, *Nanoscale,* 2009, **1**, 382-386; (j) K. T. Al-Jamal, A. Nunes, L. Methven, H. Ali-Boucetta, S. Li, F. M. Toma, M. A. Herrero, W. T. Al-Jamal, H. M. ten Eikelder, J. Foster, S. Mather, M. Prato, A. Bianco and K. Kostarelos, *Angew. Chem. Int. Ed.*, 2012,

**124**, 6495-6499; (k) H. Ali-Boucetta, A. Nunes, R. Sainz, M. A. Herrero, B. Tian, M. Prato, A. Bianco and K. Kostarelos, *Angew. Chem. Int. Ed.*, 2013, **52**, 2274-2278.

3 (a) R. Wang, J. Sun, L. Gao and J. Zhang, *J. Mater. Chem.,* 2010, **20**, 6903–6909; (b) P. He, S. Li and L. Dai, *Synth. Met.,* 2005, **154**, 17–20; (c) E. K. Hobbie, B. J. Bauer, J. Stephens, M. L. Becker, P. McGuiggan, S. D. Hudson and H. Wang, *Langmuir,* 2005, **21**, 10284-10287; (d) J. N. Barisci, M. Tahhan, G. Wallace, G. S. Badaire, T. Vaugien, M. Maugey and P. Poulin, *Adv. Func. Mater,* 2004, **14**, 133-138.

4 (a) N. W. S. Kam, M. O'Connell, J. A. Wisdom and H. Dai, *Proc. Natl. Acad. Sci. USA,* 2005, **102**, 11600-11605; (b) W. Cheung, F. Pontoriero, O. Taratula, A. M. Chen and H. He, *Adv. Drug Delivery Rev.,* 2010, **62**, 633–649; (c) S. Foillard, G. Zuber and E. Doris, *Nanoscale,* 2011, **3**, 1461-1464.

5 (a) C. Staii, M. Chen, A. Gelperin and A. T. Johnson, *Nano Lett.* 2005, **5**, 1774-1778; (b) A. Star, E. Tu, J. Niemann, J.-C. P. Gabriel, S. Joiner and C. Valcke, *Proc. Natl. Acad. Sci. USA,* 2006, **103**, 921-926; (c) P. Avouris, Z. Chen and V. Perebeinos, *Nat. Nanotechnol.,* 2007, **2**, 605-615; (d) D. A. Heller, S. Baik, T. E. Eurell and M. S. Strano, *Adv. Mater.,* 2005, **17**, 2793–2799; (e) M. Abdolahad, M. Janmaleki, M. Taghinejad, H. Taghnejad, F. Salehia and S. Mohajerzadeh, *Nanoscale*, 2013, **5**, 3421-3427.

6 (a) X. Tu, S. Manohar, A. Jagota and M. Zheng, *Nature* 2009, **460**, 250-253; (b) M. C. Hersam, *Nat. Nanotechnol.,* 2008, **3**, 387-394; (c) X. Tu and M. Zheng, *Nano Res.,* 2008, **1**, 185-194; (d) S. S. Kim, C. L. Hisey, Z. Kuang, D. A. Comfort, B. L. Farmer and R. R. Naik, *Nanoscale*, 2013, **5**, 4931-4936.

7 M. Zheng, A. Jagota, M. S. Strano, A. P. Santos, P. Barone, S. G. Chou, B. A. Diner, M. S. Dresselhaus, R. S. Mclean, G. B. Onoa, G. G. Samsonidze, E. D. Semke, M. Usrey and D. J. Walls, *Science* **2003**, *302*, 1545-1548.

8 (a) D. Roxbury, A. Jagota and J. Mittal, *J. Am. Chem. Soc.,* 2011, **133**, 13545-13550; (b) Y. Noguchi, T. Fujigaya, Y. Niidome and N. Nakashima, *Chem. Phys. Lett.,* 2008, **455**, 249-251.

9 N. Nakashima, S. Okuzono, H. Murakami, T. Nakai and K. Yoshikawa, *Chem. Lett.,* 2003, **32**, 456-457. 28a: Y. Yamamoto, T. Fujigaya, Y. Niidomea and N. Nakashima, *Nanoscale,* 2010, **2**, 1767–1772.

10 (a) Y. Song, L. Feng, J. Ren and X. Qu, *Nucleic Acids Res.,* 2011, **39**, 6835–6843; (b) C. Zhao, K. Qu, C. Xu, J. Ren and X. Qu, *Nucleic Acids Res.* 2011, **39**, 3939 - 3948.

11 (a) X. Li, Y. Peng, J. Ren and X. Qu, *Proc. Natl. Acad. Sci. USA,* 2006, **103**, 19658–19663; (b) Y. Peng, X. Wang, Y. Xiao, L. Feng, C. Zhao, J. Ren and X. Qu, *J. Am. Chem. Soc.,* 2009, **131**, 13813-13818; (c) E. Cheng, Y. Li, Z. Yang, Z. Deng and D. Liu, *Chem. Commun.*, 2011, **47**, 5545-5547.

12 P. F. Xu, H. Noh, J. H. Lee and J. N. Cha, *Phys. Chem. Chem. Phys.,* 2011, **13**, 10004–10008.

13 (a) E. Cheng, Y. Yang and D. Liu, *J. Nanosci. Nanotechnol.,* 2010, **10**, 7282–7286; (b) S. R. Shin, C. K. Lee, S. H. Lee, S. I. Kim, G. M. Spinks, G. G. Wallace, I. So, J.-H. Jeong, T. M. Kang and S. Kim, *Chem. Commun.* 2009, 1240–1242.

14 W. Chen, C. H. Tzang, J. Tang, M. Yang and S. T. Lee, *Appl. Phys. Lett.,* 2005, **86**, 103114-103116.

15 D.-H. Jung, B. H. Kim, Y. K. Ko, M. S. Jung, S. Jung, S. Y. Lee and H.-T. Jung, *Langmuir,* 2004, **20**, 8886-8891.

16 C.-L. Chung, C. Gautier, S. Campidelli and A. Filoramo, *Chem. Commun.*, 2010, **46**, 6539–6541.

17 X. Han, Y. Li, S. Wu and Z. Deng, *Small,* 2008, **4**, 326–329.

18 C. Zhao, K. Qu, Y. Song, C. Xu, J. Ren and X. Qu, *Chem. Eur. J.,* 2010, **16**, 8147-8154.

19 S. Jung, M. Cha, J. Park, N. Jeong, G. Kim, C. Park, J. Ihm and J. Lee, *J. Am. Chem. Soc.,* 2010, **132**, 10964-10966.

20 (a) R. Yang, Z. Tang, J. Yan, H. Kang, Y. Kim, Z. Zhu and W. Tan, *Anal. Chem.,* 2008, **80**, 7408–7413; (b) Y. Wan, G. Liu, X. Zhu and Y. Su, *Chem. Cent. J.* 2013, **7**, 14-19.

21 (a) S. Bhattacharya and J. Biswas, *Nanoscale*, 2011, **3**, 2924-2930; (b) S. Bhattacharya, A. Srivastava and A. Pal, *Angew. Chem. Int. Ed.*, 2006, **45**, 2934-2937; (c) S. Bhattacharya and A. Srivastava, *Langmuir*, 2003, **19**, 4439-4447.

22 R. Voggu, K. V. Rao, S. J. George and C. N. R. Rao, *J. Am. Chem. Soc.*, 2010, **132**, 5560–5561.

23 G. Hong, M. Zhou, R. Zhang, S. Hou, W. Choi, Y. S. Woo, J.-Y. Choi, Z. Liu and J. Zhang, *Angew. Chem. Int. Ed.*, 2011, **50**, 6819–6823.

24 X. Huang, R. S. Mclean and M. Zheng, *Anal. Chem.*, 2005, **77**, 6225-6228.

25 S. Ghosh, S. M. Bachilo and R. B. Weisman, *Nat. Nanotechnology,* 2010, **5**, 443-450.

26 H. Liu, D. Nishide, T. Tanaka and H. Kataura, *Nat. Commun.* 2011, **2**, 309-8pp.

27 W. Wang, K. A. S. Fernando, Y. Lin, M. J. Meziani, L. M. Veca, L. Cao, P. Zhang, M. M. Kimani and Y.-P. Sun, *J. Am. Chem. Soc.,* 2008, **130**, 1415-1419.

28 Y. Maeda, S. Kimura, M. Kanda, Y. Hirashima, T. Hasegawa, T. Wakahara, Y. Lian, T. Nakahodo, T. Tsuchiya, T. Akasaka, J. Lu, X. Zhang, Z. Gao, Y. Yu, S. Nagase, S. Kazaoui, N. Minami, T. Shimizu, H. Tokumoto and R. Saito, *J. Am. Chem. Soc.,* 2005, **127**, 10287-10290.

29 Y. Wang, H. Shan, R. H. Hauge, M. Pasquali and R. E. Smalley, *J. Phys. Chem. B,* 2007, **111**, 1249-1252.

30 L. Huang, H. Zhang, B. Wu, Y. Liu, D. Wei, J. Chen, Y. Xue, G. Yu, H. Kajiura and Y. Li, *J. Phys. Chem. C*, 2010, **114**, 12095–12098.

31 B. White, S. Banerjee, S. O'Brien, N. J. Turro and I. P. Herman, *J. Phys. Chem. C*, 2007, **111**, 13684-690.

32 S. Chakraborty, S. Sharma, P. K. Maiti and Y. Krishnan, *Nucleic Acids Res.,* 2009, **37**, 2810-2817.

33 S. Saha, K. Chakraborty and Y. Krishnan, *Chem. Commun.,* 2012, **48**, 2513-2515.

34 C. Wang, Y. Tao, F. Pu, J. Ren and X. Qu, *Soft Matter,* 2011, **7**, 10574-10576.

35 J.-L, Leroy, M. Gueron, J.-L. Mergny and C. Helene, *Nucleic Acids Res.,* 1994, **22**, 1600-1606.

36 G. Manzini, N. Yathindra and L. E. Xodo, *Nucleic Acids Res.,* 1994, **22**, 4634-4640.

37 (a) V. Verdolino, R. Cammi, B. H. Munk and H. B. Schlegel, *J. Phys. Chem. B*, 2008, **112**, 16860–16873; (b) N. Russo, M. Toscano, A. Grand and F. Jolibois, *J. Comput. Chem.*, 1998, **19**, 989-1000; (c) W. H. Brown, *Organic Chemistry, Cengage Learning,* 2013, **p. 167**; (d) K. Utsuno and H. Uludağ, *Biophys J*., 2010, **99**, 201-207; (e) J. Reijenga, A. van Hoof, A. van Loon and B. Teunissen, *Anal. Chem. Insights*. 2013, **8**, 53-71.

38 H. Kataura, Y. Kumazawa, Y. Maniwa, I. Umezu, S. Suzuki, Y. Ohtsuka and Y. Achiba, *Synth. Met.,* 1999, **103**, 2555-2558.

39 W. Z. Wang, W. F. Li, X. Y. Pan, C. M. Li, L-J. Li, Y. G. Mu, J. A. Rogers and M. B. Chan-Park, *Adv. Funct. Mater*., 2011, **21**, 1643–1651.

40 S. Neihsial, G. Periyasamy, P. K. Samanta and S. K. Pati, *J. Phys. Chem. B,* 2012, **116**, 14754-14759.

41 (a) D. Chattopadhyay, I. Galeska and F. Papadimitrakopoulos, *J. Am. Chem. Soc.,* 2003, **125**, 3370-3375; (b) F. Lu, M. J. Meziani, L. Cao and Y.-P. Sun, *Langmuir,* 2011, **27**, 4339-4350; (c) T. Tanaka, H. Jin, Y. Miyata, S. Fujii, H. Suga, Y. Naitoh, T. Minari, T. Miyadera, K. Tsukagoshi and H. Kataura, *Nano Lett.,* 2009, **9**, 1497-1500; (c) S.-Y. Ju, M. Utz and F. Papadimitrakopoulos, *J. Am. Chem. Soc.*, 2009, **131**, 6775–6784; (d) S. Toyoda, Y. Yamaguchi, M. Hiwatashi, Y. Tomonari, H. Murakami and N. Nakashima, *Chem. Asian J.,* 2007, **2**, 145–149; (e) H. Li, B. Zhou, Y. Lin, L. Gu, W. Wang, K. A. S. Fernando, S. Kumar, L. F. Allard and Y.-P. Sun, *J. Am. Chem. Soc.,* 2004, **126**, 1014-1015.